SANDIA REPORT

2013-6818
Unlimited Release
Printed August 2013

Modeling Tin Whisker Growth

Christopher R. Weinberger

Prepared by
Sandia National Laboratories
Albuquerque, New Mexico 87185 and Livermore, California 94550

Sandia National Laboratories is a multi-program laboratory managed and operated by Sandia Corporation,
a wholly owned subsidiary of Lockheed Martin Corporation, for the U.S. Department of Energy's
National Nuclear Security Administration under contract DE-AC04-94AL85000.

Approved for public release; further dissemination unlimited.

Sandia National Laboratories

Issued by Sandia National Laboratories, operated for the United States Department of Energy by Sandia Corporation.

NOTICE: This report was prepared as an account of work sponsored by an agency of the United States Government. Neither the United States Government, nor any agency thereof, nor any of their employees, nor any of their contractors, subcontractors, or their employees, make any warranty, express or implied, or assume any legal liability or responsibility for the accuracy, completeness, or usefulness of any information, apparatus, product, or process disclosed, or represent that its use would not infringe privately owned rights. Reference herein to any specific commercial product, process, or service by trade name, trademark, manufacturer, or otherwise, does not necessarily constitute or imply its endorsement, recommendation, or favoring by the United States Government, any agency thereof, or any of their contractors or subcontractors. The views and opinions expressed herein do not necessarily state or reflect those of the United States Government, any agency thereof, or any of their contractors.

Printed in the United States of America. This report has been reproduced directly from the best available copy.

Available to DOE and DOE contractors from
U.S. Department of Energy
Office of Scientific and Technical Information
P.O. Box 62
Oak Ridge, TN 37831

Telephone:	(865) 576-8401
Facsimile:	(865) 576-5728
E-Mail:	reports@adonis.osti.gov
Online ordering:	http://www.osti.gov/bridge

Available to the public from
U.S. Department of Commerce
National Technical Information Service
5285 Port Royal Rd
Springfield, VA 22161

Telephone:	(800) 553-6847
Facsimile:	(703) 605-6900
E-Mail:	orders@ntis.fedworld.gov
Online ordering:	http://www.ntis.gov/help/ordermethods.asp?loc=7-4-0#online

2013-6818
Unlimited Release
Printed August 2013

Modeling Tin Whisker Growth

Christopher R. Weinberger
Computational Materials and Data Science Department
Sandia National Laboratories
P.O. Box 5800
Albuquerque, NM 87185-0899
crweinb@sandia.gov

Abstract

Tin, lead, and lead-tin solders are the most commonly used solders due to their low melting temperatures. However, due to the toxicity problems, lead must now be removed from solder materials. This has lead to the re-emergence of the issue of tin whisker growth. Tin whiskers are a microelectronic packaging issue because they can lead to shorts if they grow to sufficient length. However, the cause of tin whisker growth is still not well understood and there is lack of robust methods to determine when and if whiskering will be a problem. This report summarizes some of the leading theories on whisker growth and attempts to provide some ideas towards establishing the role microstructure plays in whisker growth.

Acknowledgment

The author would like to acknowledge contributions from Don Susan, Joe Michael and Corbett Battaile.

Contents

Nomenclature **8**

1 Introduction **9**

2 Background **11**

3 The Role of Elastic and Plastic Anisotropy **15**

Elastic Anisotropy 15

Plastic Anisotropy 17

4 Interatomic Potentials for Tin **21**

MEAM 21

Tersoff 22

5 Discussion **25**

References **26**

List of Figures

2.1 (a) The distribution of whiskers of radii r_o with the separation of R for the model of Tu [32]. (b) The whisker modeled in [4] demonstrating the regions of plastic flow and the regions of diffusion. (c) A model of a surface grain and the definition of the angle θ suggested by [27]. 12

3.1 A plot of the average biaxial modulus of tin over the standard unit triangle. 17

3.2 The Biaxial projection factors for $\beta-$tin using the slip systems suggested by [6, 31]. 19

List of Tables

4.1 MEAM parameters given in ref. [25]. 21

4.2 A comparison of our computed values and those listed in ref. [25]. 22

4.3 Various Tersoff interatomic potential parameters for pure tin. 23

4.4 A comparison of the computed Tersoff values and literature values 24

Nomenclature

MD Molecular Dynamics

EAM Embedded Atom Method

MEAM Modified Embedded Atom Method

ODE Ordinary Differential Equation

FEM Finite Element Method

Chapter 1

Introduction

The growth of long metallic filaments, commonly called whiskers, is a long standing problem in the reliability of microelectronic packaging [5]. Whiskers tend to grow in stressed films and can reach very long lengths creating the potential to short out the electronics. It is equally well known that creating a lead-tin solder mitigates the whisker growth problem. With the current drive to remove lead from solders both commercially and in military applications, the problem of tin whiskers has re-emerged. However, there is no current agreed upon understanding of why whiskers grow or why adding lead alleviates the problem.

The goal of this project was to understand what role the tin microstructure plays in determining which grains will grow into a whisker. Only certain grains, one in thousands, will grow into a whisker and if we can determine which grains grow in to whiskers, it may be possible to engineer the microstructure to limit growth. While the understanding of tin whisker formation is not complete, it is generally agreed upon that diffusion is responsible for whisker growth, which occurs under compressive stresses. However, due to the limited time frame of the project, only some very basic ideas were investigated. Specifically, this report will cover some of the basic models of whisker growth and will present some ideas about elastic and plastic anisotropy in tin. This report also provides a short evaluation of the current interatomic potentials for tin which may be useful in understanding diffusion and plastic anisotropy.

Chapter 2

Background

Whiskers have been known to grow from tin thin films as early as the 1950's [5, 12, 19] and are a known reliability issue for the microelectronics industry [5]. While a significant amount of research was conducted in this area [2, 7, 15, 23], the mitigation strategy of using lead-tin solders was identified [3, 8, 9] and reduced the problem of whiskering. With the addition of lead to tin, the interest in whisker growth diminished until legislation in various countries banned lead from solders.

The purpose of this section is to provide some background for the modeling of tin whisker growth. For a complete review of the pre-2004 literature on tin whisker growth, the reader is referred to a nice review article by Galyon [16]. The relevant points to make are in regards to the driving forces required and the mechanisms of whisker growth. The earliest theories associated with tin whisker growth involve dislocation theory [10, 13, 14, 28, 29]; a theory that it is now discounted by most researchers. Most modern theories of whisker growth [4, 21, 24, 27, 32, 33] are associated with diffusion, usually through the grain boundaries, with stress or stress gradients as the driving force.

The first model worth discussing is the one introduced by Tu [32] and is often regarded as the first stress-assisted diffusion model of tin whisker growth. The model is based on stress-assisted diffusion with the chemical potential, μ, approximated by the product of the stress and the atomic volume of tin. In this case, the chemical pontential is:

$$\mu = \sigma\Omega \tag{2.1}$$

The flux of atoms is then given by a generalization of Fick's Law stating that the flux is the diffusivity, D, times the concentration, C divided by $k_B T$ times the gradient of the chemical potential:

$$\mathbf{J} = -\frac{DC}{k_B T}\nabla\mu \tag{2.2}$$

which, for the assumed chemical potential, is:

$$\mathbf{J} = -\frac{DC}{k_B T}\Omega\nabla\sigma \tag{2.3}$$

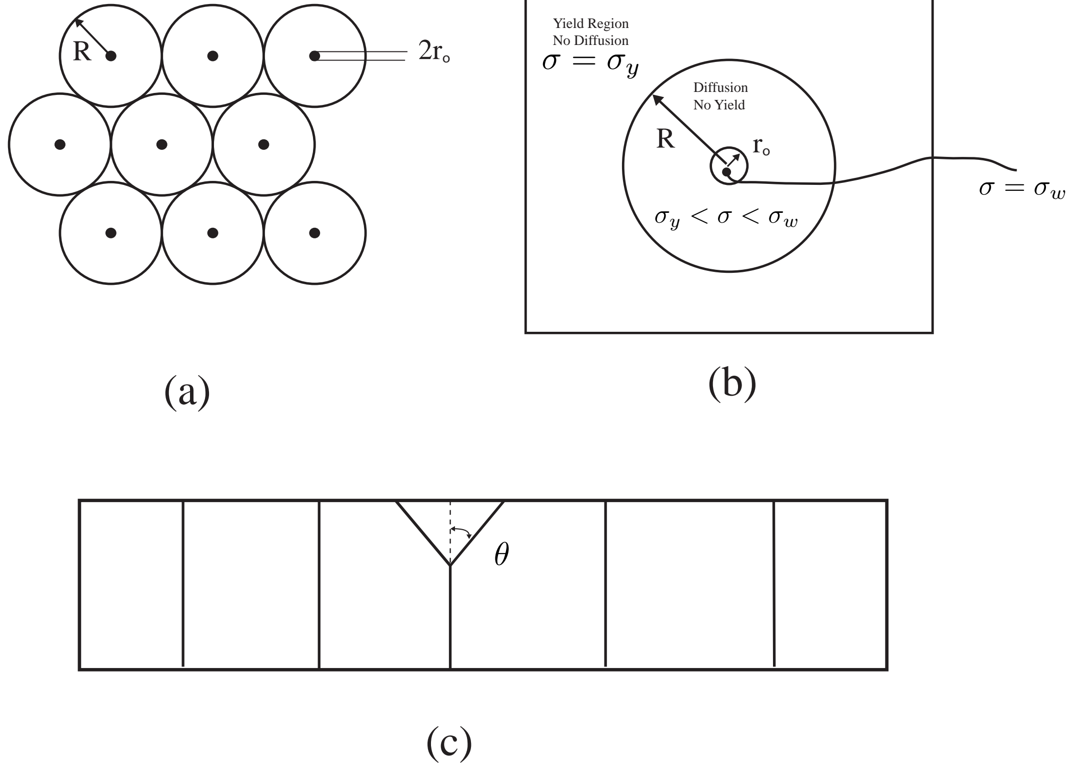

Figure 2.1. (a) The distribution of whiskers of radii r_o with the separation of R for the model of Tu [32]. (b) The whisker modeled in [4] demonstrating the regions of plastic flow and the regions of diffusion. (c) A model of a surface grain and the definition of the angle θ suggested by [27].

This demonstrates that the flux of atoms occurs in the direction of deceasing stress. Thus, a stress gradient is required for mass diffusion to occur and can be thought of as the thermodynamic driving force for mass transport. The second part of the model assumes that mass continuity holds in cylindrical region around the whisker of radius r_o where the stress is assumed to be zero and a region outside the whisker, R where the stress is assumed to be the biaxial applied stress, σ_o. For simplicity, this region is assumed to be cylindrical, as that shown in Figure 2.1(a).

Mass continuity requires that $\nabla \cdot \mathbf{J} = 0$ and in cylindrical coordinates, this reduces to the ODE for σ as:

$$\nabla^2 \sigma = 0 \tag{2.4}$$

$$\frac{1}{r}\frac{d\sigma}{dr} + \frac{d^2\sigma}{dr^2} = 0 \tag{2.5}$$

which admits the solution:

$$\sigma = A \ln \frac{r}{r_o} + B \tag{2.6}$$

with the boundary conditions that $\sigma|_{r=r_o} = 0$ and $\sigma|_{r=R} = \sigma_o$. Using the boundary conditions, the stress is:

$$\sigma = \sigma_o \frac{\ln(r/r_o)}{\ln(R/r_o)} \tag{2.7}$$

and the flux is:

$$J = \frac{-DC}{k_B T} \frac{\sigma_o \Omega}{\ln(R/r_o)} \frac{1}{r} \tag{2.8}$$

Noting that the concentration $C = \Omega^{-1}$, the flux is simply $J = \frac{-D}{k_B T} \frac{\sigma_o}{\ln(R/r_o)} \frac{1}{r}$. Thus, the mass transport into the whisker, at $r = r_o$, in a time Δt is:

$$JA\delta t\Omega = \pi r_o^2 \delta h \tag{2.9}$$

where $A = 2\pi r_o s$ is the area at the base of the whisker where the mass flows into and the authors take s to be the step height (although other choices are equally logical [17, 27]). Thus, the rate of the growth of the whisker is:

$$\frac{\Delta h}{\Delta t} = \frac{2}{\ln(R/r_o)} \frac{\sigma_o \Omega s D}{k_B T r_o^2} \tag{2.10}$$

Hutchinson *et al.* [17] provides a very similar model with only minor modifications in terms of the constants used. This basic model has been modified by several other authors [4, 27] to account for the effects of plasticity or surface grains. One of the key aspects of this model is the choice of the outer Radii R. Tu assumes that the spacing is controlled by cracks or weak spots in the oxide. This radius is important because it helps determine the mangnitude of the growth rate of whiskers.

This simple model has been modified by Buchovecky *et al.* [4] to include a mass generation term, which accounts for the stress generation rate in the film, to match their finite element simulations. The authors assume that the film is plastically deforming in areas outside the whisker and have a yield stress of σ_y while the whisker grain has a yield stress of σ_w. The model further assumes that in a region R, the film does not yield but allows for diffusion to the whisker while the region outside R plastically deforms but does not allow diffusion as illustrated in Figure 2.1(b). Continuity then becomes:

$$\frac{1}{r}\frac{d\sigma}{dr} + \frac{d^2\sigma}{dr^2} = \frac{2}{3}\dot{e} k_B T \tag{2.11}$$

with the boundary conditions $\sigma|_{r=r_o} = \sigma_w$ and $\sigma|_{r=R} = \sigma_y$. The ODE has the solution:

$$\sigma = (\sigma_y - \sigma_w)\frac{\ln(r/r_o)}{\ln(R/r_o)} + \frac{1}{6}\frac{\dot{e}k_B T}{D}\left[\left(r_o^2 - R^2\right)\frac{\ln(r/r_o)}{\ln(R/r_o)} + r^2 - r_o^2\right] + \sigma_w \tag{2.12}$$

The region R over which diffusion occurs is now set by the condition that $\frac{d\sigma}{dr}\big|_{r=R} = 0$, which says that there is no mass transfer between the outer plastically deforming region and the diffusion region. This also allows for a simple determination of the whisker growth rate:

$$\frac{\Delta h}{\Delta t} = \frac{2}{3}\dot{e}(R^2 - r_o^2)h_f \tag{2.13}$$

where h_f is the thickness of the film. One of the key results here is that the whisker spacing is not assumed and has no role in the solution. Instead, the distance R is set by the extent of diffusion. However, if the spacing is too small, the diffusion regions overlap and this simple model is invalid, as was demonstrated using FEM simulations.

Sarabol *et al.* modify the model by Tu [32] by adding a back stress term that accounts for the friction associated with grain boundary sliding. The effect of this term is that it makes whisker growth occur only from surface grains or grains with inclined boundaries as shown in Figure 2.1(c). This supports a common notion that columnar grains cannot grow into whiskers. The modified whisker growth equation suggested by Sarabol *et al.* is:

$$\frac{\Delta h}{\Delta t} = \frac{2}{\ln(R/r_o)}\frac{\Omega s D}{k_B T r_o^2}\left[\sigma_o - \frac{\beta}{\tan\theta}\right] \tag{2.14}$$

where β is the coefficient for grain boundary sliding, i.e. $F_{slide} = \beta A_{slide}$.

These basic models provide insight into the physics behind whisker growth. However, the models do not provide us with a clear criteria for selecting a grain that will whisker. The model proposed by Sarabol *et al.* [27] suggests that only surface grains will grow, but which ones. The model also does not provide a clear method to determine the outer Radius R, which helps control growth as much as β and $\tan\theta$. The model of Buchovecky *et al.* [4] determines the outer radius R and tells us that weak grains will grow, but not what weak grains are.

As stated previously, this short report will look at some aspects of anisotropy as potential sources for stress gradients that will drive whisker growth. It will also present some basic evaluation of interatomic models that can be used to better understand diffusion and sliding in grain boundaries.

Chapter 3

The Role of Elastic and Plastic Anisotropy

In the previous section, we reviewed some of the basic theories of whisker growth. Notably, the work of Tu [32, 33] and Buchovecky *et al.* [4] have introduced a set of models for the growth of tin whiskers based on the idea of a "weak" grain. Tu [32] originally proposed that the nucleation site was associated with a crack in the tin oxide layer. Buchovecky *et al.* [4] introduced the idea that the "weak" grain was actually a grain with a lower yield strength than the surrounding grains. This introduces a general classes of "weak" grain models where mass flow occurs to grains that have low stress states.

While these models are certainly plausible, they do not provide a method to determine which grains are likely to grow into whiskers. Notably, the low yield stress model of Buchovecky *et al.* does not tell us which grains have low stress and would thereby be candidates as mass sinks. In this section, we investigate the possibility of elastic and plastic anisotropy, and hence texture, as a marker for identifying grains that are likely to grow into whiskers.

Elastic Anisotropy

In the elastic model, we will work under the basic assumptions of those invoked by Tu [32] except that we do not make the assumption that the stress is zero where a crack forms in the oxide layer. Rather, we assume that the stress is distributed in the film due to elastic anisotropy and that the "weak" grains are those with low elastic moduli. Presumably, then, these grains will act as mass sinks and diffusion will occur to these types of grains. This relies on the assumption that during straining, all the grains remain in the elastic regime; an assumption that warrants investigation and has been pointed out by Buchovecky *et al.* to be implausible for isotropic films.

In the case of a simple elastic response, we assume that the tin film is subjected to a constant biaxial strain rate, $\dot{\varepsilon}$. In an isotropic film this results in a biaxial stress rate:

$$\dot{\sigma} = M\dot{\varepsilon} \tag{3.1}$$

where M is the biaxial modulus of the material. In the case that the film is anisotropic, the stress will distribute through the film according using the anisotropic elasticity tensor such that $\sigma_{ij} = C_{ijkl}\varepsilon_{kl}$. If, however, the material is anisotropic and polycrystalline, the stress distribution will

depend on the texture of the film and the elastic constants of the film. Such stress distributions can be solved using standard finite element codes. However, these solutions can be time consuming, depend on the grain structure and do not provide a convenient method to interpret experimental data.

A single parameter that approximates the stress accumulation in the grain under biaxial deformation would be very useful metric. If the film were subjected to uni-axial deformation, this parameter would be the Young's modulus of the grain and can be computed from the elastic compliance tensor oriented along the tensile axis. However, in this case we have biaxial deformation. Here, we approximate the biaxial modulus of the film from elastic anisotropy of the grain. To construct this average biaxial modulus, we assume that the film is subjected to biaxial strain: $\varepsilon_{11} = \varepsilon_{22} = \varepsilon$, $\sigma_{33} = 0$, and all the shear strains are zero: $\varepsilon_{12} = \varepsilon_{13} = \varepsilon_{23} = 0$. This results in the following stress-strain equations using standard anisotropic elasticity:

$$\sigma_{11} = C_{11}\varepsilon + C_{12}\varepsilon + C_{13}\varepsilon_{33} \tag{3.2}$$

$$\sigma_{22} = C_{22}\varepsilon + C_{12}\varepsilon + C_{23}\varepsilon_{33} \tag{3.3}$$

$$\sigma_{33} = C_{13}\varepsilon + C_{23}\varepsilon + C_{33}\varepsilon_{33} = 0 \tag{3.4}$$

which, upon solving for σ_{11} and σ_{22} results in:

$$\sigma_{11} = \left(C_{11} + C_{12} - \frac{C_{13} + C_{23}}{C_{33}} C_{13}\right)\varepsilon \tag{3.5}$$

$$\sigma_{22} = \left(C_{12} + C_{22} - \frac{C_{13} + C_{23}}{C_{33}} C_{23}\right)\varepsilon \tag{3.6}$$

This result demonstrates that there is no easy definition of a biaxial modulus for the general anisotropic case as, in general, $C_{11} \neq C_{22}$ and $C_{13} \neq C_{23}$. This is true even in materials with high symmetry, such as cubic crystals, because the elastic constants used here are with respect to the loading axis and not standard crystallographic axes. Thus, even in a cubic crystal, the stress in the film will not be purely biaxial even if the strain state is. However, we can define an average biaxial modulus which relates the average stress in the crystal to the biaxial strain as:

$$\overline{M} \equiv \frac{\overline{\sigma}}{\varepsilon} \tag{3.7}$$

where $\overline{\sigma} \equiv \frac{1}{2}(\sigma_{11} + \sigma_{22})$. Thus, the approximate biaxial modulus $\overline{M}$ can be defined as

$$\overline{M} = \frac{1}{2}\left(C_{11} + C_{22} + 2C_{12} - \frac{(C_{13} + C_{23})^2}{C_{33}}\right) \tag{3.8}$$

It is worth pointing out that the definition of $\overline{M}$ depends on the normal direction, but not the in-plane directions. This makes $\overline{M}$ a good measure of the average biaxial stress in the film and, as such, a good measure of the anisotropic response of a single grain to a biaxial strain.

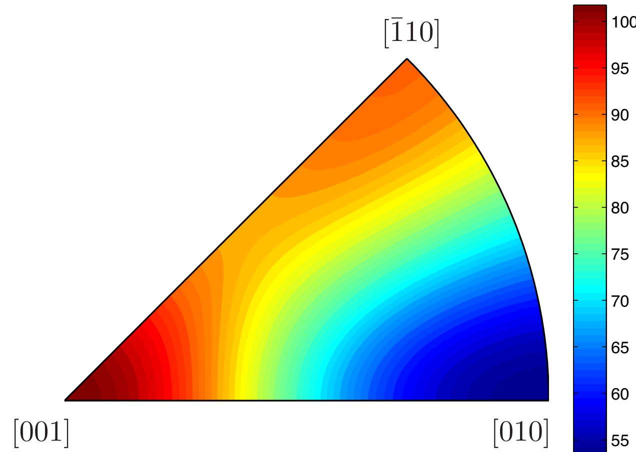

Figure 3.1. A plot of the average biaxial modulus of tin over the standard unit triangle.

To see how $\overline{M}$ can be useful, lets assume a polycrystalline film is subjected to biaxial strain ε (or strain rate $\dot{\varepsilon}$). The the stress (or stress rate) can be approximated in each grain as $\overline{\sigma} = \overline{M}\varepsilon$. Thus, the variation of $\overline{M}$ can be thought of as the variation of stress in a polycrystalline film under biaxial stress. This construct would be similar to using the Young's modulus of a single grain (where $E \equiv S^{-1}_{1111}$.) to determine the stress in each grain for a polycrystalline bar subjected to uniaxial tension.

To apply this to $\beta-$tin, we need the elastic constants of the body-centered-tetragonal crystal. There are a number of references that cite elastic constants for tin. Using the values of Rayne and Chandrasekhar [26], we plot $\overline{M}$ over the unit triangle as illustrated in Figure 3.1. From this plot, we can see the modulus is low near the [010] pole and high along the side of the triangle that connects the [001] to the [$\bar{1}$10] pole.

Plastic Anisotropy

Plastic anisotropy plays a major role in accumulated plastic strain and texture evolution in polycrystals and has the potential to contribute significantly to whisker growth. Notably, Buchovecky *et al.* [4] has demonstrated that whisker growth will occur in grains that have low flow stresses compared to an extended neighborhood of grains. This demonstrates that the existence of plastically weaker grains may control whisker growth and one obvious reason a grain may be weak is through plastic anisotropy.

However, the major limitation in understanding plastic anisotropy in white tin is that the slip systems in white tin are not well established. The slip systems in tin are difficult to identify

because of the complicated β−tin structure. This gives rise to a large number of possible slip systems. In addition, tin has a low melting temperature which means that, at room temperature, thermal activation may allow a large number of slip systems to be active.

A recent review article by Yang and Li [30] provides a comprehensive review of the slip systems in white tin. The slip systems included:

1. $(110)[\bar{1}11]$
2. $(110)[001]$
3. $(100)[010]$
4. $(100)[001]$
5. $(101)[\bar{1}01]$
6. $(121)[\bar{1}01]$
7. $(100)[011]$
8. $(101)[11\bar{1}]$
9. $(101)[010]$
10. $(001)[100]$
11. $(001)[110]$
12. $(121)[1\bar{1}1]$

Since the energy of a dislocation scales with the Burger's vector squared, dislocations with smaller Burgers vectors should be favored. The Burgers vectors are $b_{[001]} = 0.316$ nm, $b_{[111]} = 0.441$ nm, $b_{[100]} = 0.582$ nm, and $b_{[101]} = 0.663$ nm [30]. Thus, one would expect the $b_{[001]}$ and $b_{[111]}$ to be the favored slip directions, and this crude argument is supported by anisotropic elasticity calculations [11]. Despite this argument, dislocations with $\langle 101\rangle$, $\langle 110\rangle$ and $\langle 001\rangle$ burgers vectors have been observed and are likely required to accommodate general deformation.

Recent anisotropic crystal plasticity models [6, 31] have advocated for the use of slip systems 1-5,7,10,12 and the $(110)[\bar{1}10]$. In these models, they use a common yield stress for all the slip systems with less favorable slip systems assigned a lower hardening rate. Another approach that has been recently taken is the use of DFT to compute the ideal shear strengths different slip systems and to create a uniaxial yield law based on the DFT shear strength calculations [18]. The main slip systems identified as (by the slip system numbers listed above: 1,3,5,6,9, and 12).

The idea here is to use plastic anisotropy to determine which grains are hard, and which grains are soft in the sense of strength. If we assume, as is done in [6, 31], that each slip system has the same critical resolved shear stress, then the Schmid factor determines the relative strength of the tin

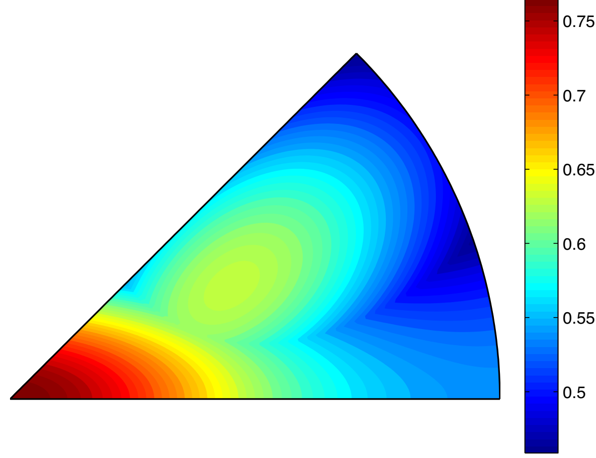

Figure 3.2. The Biaxial projection factors for $\beta-$tin using the slip systems suggested by [6, 31].

grains in uniaxial tension. However, the loading in the tin whisker problem is not uniaxial tension and thus we need a stress projection, factor similar to the Schmid factor, for biaxial loading. A generalized Schmid factor can be created by considering the contraction of the applied stress tensor and the Schmid tensor. The Schmid tensor is defined as the symmetric part of the dyadic product of the slip plane normal and Burgers vector (normalized):

$$\mathbf{M} \equiv \frac{1}{2}\left(\mathbf{n}\otimes\mathbf{b}+\mathbf{b}\otimes\mathbf{n}\right) \tag{3.9}$$

where **n** and **b** are the normalized slip plane normal and normalized Burgers vector. The generalized Schmid factor can now be defined as $M^* \equiv \sigma/||\sigma||_2 : \mathbf{M}$, where σ is the applied stress tensor and $||A||_2$ denotes the 2-norm of A. If the applied stress is a biaxial stress, then the generalized Schmid Factor can be thought of as the Biaxial Schmid factor which, assuming that the resolved shear stress on each system is the same, provides a map of the strong and weak grains.

Figure 3.2 shows the variation of the Schmid factor over the unit triangle in $\beta-$tin using the active slip systems of [6, 31]. However, experiments on the yield stress in $\beta-$tin suggest that a model of constant shear strength across the slip systems is likely inappropriate for $\beta-$tin [20]. Similar conclusions can be obtained from computer modeling [18]. If the the systems have different critical resolve shear stresses, the Schmid factor plot in Figure 3.2 is inappropriate to describe the plastic anisotropy. In order to evaluate the role plastic anisotropy plays in determining the whisker growth, extensive work is needed in determining the critical resolved shear stress in $\beta-$tin beyond what is currently known.

Chapter 4

Interatomic Potentials for Tin

In this section we will review some of the interatomic potentials for tin. As previously mentioned, tin forms the $\beta-$ tin structure at room temperature and the diamond cubic structure at 3°C. As these are the two most relevant crystal structures for tin and each structure is dominated by metallic and covalent bonding, respectively, we need potentials that can capture both types of bonding. One such potential is the Modified Embedded Atom Method (MEAM), which has been specifically developed to handle both solid phases as well as the liquid properties of tin. Another candidate potential to describe tin is the general form introduced by Tersoff which is commonly used to describe ceramics and metals.

MEAM

The MEAM formulation is an extension of the well known embedded atom method (EAM) developed by Baskes, Daw and Foiles. The MEAM formulation continues the ideas of representing the total energy of a system of atoms using a pair potential and an embedding function as:

$$E = \sum_{i} F_i\left(\bar{\rho}_i\right) + \frac{1}{2}\sum_{i \neq j} S_{ij}\phi_{ij}\left(r_{ij}\right) \tag{4.1}$$

where F_i is the embedding function for an atom i with electron density $\bar{\rho}_i$, S_{ij} is the screening function and $\phi_{ij}\left(r_{ij}\right)$ is the pair interaction between atoms i and j separated by a distance r_{ij}. The MEAM potential has been parameterized specifically for grey and white tin [25]. We have taken the parameters listed in the paper, see Table 4.1, and tested them out in LAMMPS against elastic properties and structural energies. The values computed here are listed against those reported in the paper and we do see some differences, as shown in Table 4.2.

Table 4.1. MEAM parameters given in ref. [25].

E_c	A	r_o (Å)	α	$\beta^{(0)}$	$\beta^{(1)}$	$\beta^{(2)}$	$\beta^{(3)}$	$t^{(1)}$	$t^{(2)}$	$t^{(3)}$
3.08	1.0	3.44	6.20	6.2	6.0	6.0	6.0	4.5	6.5	-0.183

Table 4.2. A comparison of our computed values and those listed in ref. [25].

Property	Units	This Work	Ref. [25]
$\beta-$Sn			
E_{coh}	eV	3.085	3.085
a	Å	5.9251	5.8313
c/a		0.546	0.546
C_{11}	GPa	111.3	109.4
C_{33}	GPa	139.1	107.8
C_{12}	GPa	64.6	57.7
C_{13}	GPa	24.9	34.8
C_{44}	GPa	23.5	26.8
C_{66}	GPa	0.84	2.56
$\alpha-$Sn			
E_{coh}	eV	3.14	3.14
a	Å	6.492	6.483
C_{11}	GPa	71.8	73.4
C_{12}	GPa	30.0	26.6
C_{44}	GPa	36.6	39.1

Tersoff

The MEAM potential appears to be one of the few potentials that has been rigorously fit to both grey and white tin properties. An alternative potential that is capable of representing both metals and ceramics is the Tersoff potential. Following the notation introduced in LAMMPS (http://lammps.sandia.gov), the energy of a group of atoms described by the general Tersoff potential is:

$$E = \frac{1}{2}\sum_{i}\sum_{j\neq i} V_{ij} \quad (4.2)$$

$$V_{ij} = f_C(r_{ij})\left[f_R(r_{ij}) + b_{ij} f_A(r_{ij})\right] \quad (4.3)$$

$$f_C = \begin{cases} 1 & : \; r < R-D \\ \frac{1}{2} - \frac{1}{2}\sin\left(\frac{\pi}{2}\frac{r-R}{D}\right) & : \; R-D < r < R+D \\ 0 & : \; r > R+D \end{cases} \quad (4.4)$$

$$f_R(r_{ij}) = A\exp\left(-\lambda_1 r\right) \quad (4.5)$$

$$f_A(r_{ij}) = -B\exp\left(-\lambda_2 r\right) \quad (4.6)$$

$$b_{ij} = \left(1+\beta^n\zeta_{ij}^n\right)^{-\frac{1}{2n}} \quad (4.7)$$

$$\zeta_{ij} = \sum_{k\neq i,j} f_C(r_{ik})\, g(\theta_{ijk}) \exp\lambda_3^m \left(r_{ij}-r_{ik}\right)^m \quad (4.8)$$

Table 4.3. Various Tersoff interatomic potential parameters for pure tin.

Parameter	Berroukche *et al.* [1]
m	3.0
γ	1.00
λ_3	0.0
c	101266.29
d	15.590
$\cos\theta_0$	-0.43822
n	0.75003
β	9.64E-7
λ_2	1.6424
B	537.67
R	3.2
D	0.15
λ_1	2.3548
A	2740.30

$$g(\theta) = \gamma_{ijk}\left(1+\frac{c^2}{d^2}-\frac{c^2}{\left[d^2+(\cos\theta-\cos\theta_0)^2\right]}\right) \tag{4.9}$$

The potential has a three body term and thus includes atoms as the sums occur over all the the j and k neighbors of atom i.

There are a number of Tersoff potentials that have been developed, but some are not fit to whit tin or we have been unable to reproduce the potential behavior appropriately. Umeno and Negami [34] fit a tersoff potential to both grey and white tin with an emphasis on studying diffusion with applications to tin whiskers. After implementation of the potential in LAMMPS, we found that the lattice constants were close to those published in the paper, but the cohesive energies could not be reproduced reasonably. Alternatively, a Tersoff potential was fit by Berroukche *et al.* [1] to grey tin. This potential represents some of the properties of white tin relatively well (see Table 4.4. Note that C_{33} is much too large for this potential. Further optimization of Tersoff potentials may prove useful in simulating the properties of grey (β) tin.

Table 4.4. A comparison of the computed Tersoff values and literature values

Property	Units	This Work (Berroukche *et al.*)	Ref. [1]
$\beta-$Sn			
E_{coh}	eV	2.895	
a	Å	5.818	
c/a		0.542	
C_{11}	GPa	146	
C_{33}	GPa	1030	
C_{12}	GPa	40.6	
C_{13}	GPa	17.5	
C_{44}	GPa	15.0	
C_{66}	GPa	16.9	
$\alpha-$Sn			
E_{coh}	eV	3.175	3.109
a	Å	6.491	6.490
C_{11}	GPa	85.6	70.1
C_{12}	GPa	33.0	38.1
C_{44}	GPa	39.3	36.8

Chapter 5

Discussion

This work reviewed some of the basic models of tin whisker growth that involve stress-assisted diffusion in tin films. Most of these models assume there are weak grains from which whiskers can grow. It is of great interest to be able to predict which one of thousands of grains will grow a whisker. This is obviously a very challenging task as there are many factors that contribute to whisker growth.

In this work, the potential role of elastic and plastic anisotropy was briefly investigated. Plastic anisotropy may be an important area to investigate in order to understand which grains are likely to grow whiskers and which do not. For example, recent work by Pei *et al.* [22] has shown that there is a tendency to form in $\langle 001 \rangle$ grains (normal to the film) that are surrounded by $\langle 010 \rangle$ grains. Using the Biaxial Schmid factor plot in Figure 3.1, we can see that $\langle 001 \rangle$ are soft and $\langle 010 \rangle$ grains are hard assuming uniform critical resolved shear stresses on the slip systems. This simple model would suggest that the $\langle 100 \rangle$ grains would yield before $\langle 010 \rangle$ grains, and following the model of Buchovecky *et al.* [4] would grow whiskers if surrounded by $\langle 010 \rangle$ grains. However, as pointed out by Pei *et al.* that some of $\langle 100 \rangle$ grains surrounded by $\langle 010 \rangle$ grains did not grow whiskers. Thus, there may be additional factors at play in determining which grains grow.

This particular example does provide evidence that plastic anisotropy may play an important role in determining which grains grow into whiskers. However, there is much we do not know about plasticity in tin. Thus, it is important to study plasticity in single and polycrystalline tin to better understand plastic anisotropy in this material to better calibrate models of tin whisker growth.

References

[1] B. S. A. Berroukche and K. Amara. Molecular dynamics simulation study of structural, elastic and thermodynamic properties of tin below 286 K. *Int. J. Nanoelectronics and Materials*, 1:41–51, 2008.

[2] S. M. Arnold. The growth and properties of metal whiskers. *Proc.* 43rd *Annual Convetion of the America Electroplater's Soc.*, pages 26–31, 1956.

[3] S. M. Arnold. The growth of metal whiskers on electrical components. *Proc. of the IEEE Elec. Comp. Conf.*, pages 75–82, 1959.

[4] E. J. Buchovecky, N. Du, and A. F. Bower. A model of Sn whisker growth by coupled plastic flow and grain boundary diffusion. *Appl. Phys. Lett.*, 94:191904, 2009.

[5] K. G. Compton, A. Mendizza, and S. M. Arnold. Filamentary growths on metal surfaces - "whiskers". *Corrosion*, 7:327–334, 1951.

[6] P. Darbandi, T. R. Bieler, F. Pourbohhrat, and T.-K. Lee. Crystal plasticity finite-element analysis of deformation behavior in multiple-grained lead-free solder joints. *J. Electron. Mater.*, 42:201–214, 2013.

[7] R. H. Doremus, B. W. Roberts, and D. Turnball, editors. *Growth of Metal Whiskers From the Solid*. John Wilely & Sons, New York, 1958.

[8] B. Dunn. Metallurgy and reliability in spacecraft electronics. *Metals and Materials*, 34:34–38, 1975.

[9] B. Dunn. Whisker formation on electronic materials. *Circuit World*, 2:32–40, 1976.

[10] J. D. Eshelby. A tentative theory of metallic whisker growth. *Phys. Rev.*, 91:755–756, 1953.

[11] R. Fiedler and I. VAGER. On the burgers vectors in $\beta-$Sn single crystals. *Phys. Stat. Sol. A*, 32:419–424, 1975.

[12] R. M. Fisher, L. S. Darken, and K. G. Carroll. Accelerated growth of tin whiskers. *Acta Metall.*, 2:368–373, 1954.

[13] F. C. Frank. On tin whiskers. *Phil. Mag.*, 44:854–860, 1953.

[14] J. Franks. Growth of whiskers in the solid phase. *Acta Metall.*, 6:103–109, 1958.

[15] V. K. Galuzunova. A study of the influence of certain factors on the growth of filamentary tin crystals. *Kristallografiya*, 7:761–768, 1954.

[16] G. T. Galyon. Annotated tin whisker bibliography and anthology. *IEEE Transactions on Electronics Packaging Manufacturing*, 28:94–122, 2005.

[17] B. Hutchinson, J. Oliver, M. Nylen, and J. Hagstrom. Whisker growth from tin coatings. *Mat. Sci. Forums*, 467-470:465–470, 2004.

[18] Y. Kinoshita, H. Matsushima, and N. Ohno. Predicting active slip systems in β-sn from ideal shear resistance. *Model. Simul. Mater. Sci. Eng.*, 20:035003, 2012.

[19] S. E. Koonce and S. M. Arnold. Growth of metal whiskers. *J. Appl. Phys.*, 24:365–366, 1954.

[20] M. Nagasaka. Temperature dependence of plastic deformation in white tin single crystals. *Jap. J. Appl. Phys.*, 28:446–452, 1989.

[21] J. W. Osenbach. Creep and its effect on sn whisker growth. *J. Appl. Phys.*, 106:094903, 2009.

[22] F. Pei, N. Jadhav, and E. Chason. Correlating whisker growth and grain structure on sn-cu samples by real- time scanning electron microscopy and backscattering diffraction characterization. *Appl. Phys. Lett.*, 100:221902, 2012.

[23] C. H. Pitt and R. G. Henning. Pressure-induced growth of metal whiskers. *J. Appl. Phys.*, 35:459–460, 1964.

[24] K. J. Puttlitz and K. A. Stalter, editors. *The Structure and Kinetics of Tin-Whisker Formation and Growth on High Tin Content Finishes*. CRC Press, New York, 2004.

[25] R. Ravelo and M. I. Baskes. Equilibrium and thermodynamic properties of grey, white, and liquid tin. *Phys. Rev. Lett.*, 79:2482–2485, 1997.

[26] J. A. Rayne and B. S. Chandrasekhar. Elastic constants of β tin from 4.2° to 300°. *Phys. Rev.*, 5:1658–1663, 1960.

[27] P. Sarobol, J. Blendell, and C. Handwerker. Whisker and hillock growth via coupled localized coble creep, grain boundary sliding, and shear induced grain boundary migration. *Acta Mat.*, 61:1991–2003, 2012.

[28] G. W. Sears. A mechanism of whisker growth. *Acta Mettal.*, 3:367–369, 1955.

[29] G. W. Sears. On the formation and properties of helical dislocations. *Phil. Mag.*, 2:355–377, 1957.

[30] K. V. Subramanian, editor. *Deformation behavior of tin and some tin alloys*. Springer, New York, 2006.

[31] L. B. T. R. Bieler, B. Zhou, A. Zamiri, P. Darbandi, F. Pourboghrat, T.-K. Lee, and K.-C. Liu. The role of elastic and plastic anisotropy of sn in recrystallization and damage evolution during thermal cycling in sac305 solder joints. *J. Electron. Mater.*, 41:283–301, 2012.

[32] K. N. Tu. Irreversible processes of spontaneous whisker growth in bimetallic Cu-Sn thin-film reactions. *Phys. Rev. B*, 49:2030–2034, 1994.

[33] K. N. Tu, C. Chen, and A. T. Wu. Stress analysis of spontaneous Sn whisker growth. *J. Mater. Sci: Mater. Electron.*, 18:269–281, 2007.

[34] Y. Umeno and J. Negami. Atomistic simulation of stress-induced grain boundary diffusion: For tin-whisker problem. *Materials Science Forum*, 706-709:1545–1549, 2012.

DISTRIBUTION:

1	MS 0889	Corbett C. Battaile, 1814
1	MS 1411	Amy C. Sun, 1814
1	MS 1411	Hojun Lim, 1814
1	MS 0899	Technical Library, 9536 (electronic copy)
1	MS 0359	D. Chavez, LDRD Office, 7911

Sandia National Laboratories